

Oil-Free Eye Drops of Cyclosporine A as a Treatment Modality for Dry Eye Disease

1. Introduction

Tear Film and Ocular Surface (TFOS) society defines dry eye disease (DED) as a multifactorial disease of tears and ocular surface which results in discomfort, visual disturbances, and tear film instability. DED results in severe inflammation due to the reduction in tear secretion or increase in tear evaporation. Approximately, 5-50% of people worldwide are suffering from DED irrespective of their age, region and other demographics^{1,2}. Currently, DED is managed by topical instillation of either artificial tears or immunomodulatory/ anti-inflammatory agents. Artificial tears, though provides immediate relief does not address the underlying condition of inflammation. Hence, chronic DED requires the dosages of corticosteroids such as methylprednisolone, loteprednol), immunosuppressants (cyclosporine A, CsA), tetracyclines (doxycycline, minocycline), and lifitegrast^{3,4}

Clinically, CsA (**Fig. 1A**) is a preferred drug for the treatment of DED as its action is specific and reversible compared to other corticosteroids and acts by inhibiting the cytokines thus preventing the T-cell activation. However, CsA is a large peptide molecule and severely limited by its poor aqueous solubility warranting a formulation as an emulsion or micelles. Therefore, the currently available formulations namely Cequa® (0.09% CsA, Sun Pharma), Restasis® (0.05% CsA, Allergan Inc.), Ikervis® (0.1% CsA, Santen Pharma) all contain oil. Due to the ocular physiology, the instillation of oil-based formulations suffers from the risk of pain, redness, irritation, headache and infections. Furthermore, CsA shows poor permeability and ocular bioavailability owing to the higher partitioning into the oil phase⁵. In this context, it is evident that a completely aqueous-based eye drops of CsA can address the concerns for an effective management of DED.

Literature reports several techniques for increasing the aqueous solubility of CsA by complexation, *in situ* gelling, or use of hydrogel contact lenses. In addition, numerous

types of nanotechnological products – either lipid or polymer-based are in exploration. Though, the novel products have shown equal or superior performance compared to the marketed formulations of CsA, one would always prefer eye drops due to its unmatched patient compliance, ease of manufacturing and scalability, and possibility of integration into the existing protocols of the industry. Therefore, in the present study an attempt was made to develop a completely particle-free aqueous formulation of CsA, in the form of eye drops to manage DED.

Cyclodextrins (CD) are well-known for their ability to hold lipophilic drugs within their hydrophobic cavity and aiding in their solubility. Out of the various derivatives of CD, sulfobutylether-beta-CD (SBE- β -CD, **Fig. 1B**) is the most promising excipient that is pharmacologically inert, safe and approved for clinical use⁶. Additionally, formulating SBE- β -CD complexes are well-established in an industrial setup, conferring high levels of stability, and ease of sterilization. Conventionally, SBE- β -CD and a drug forms a binary complex, but with the addition of a water-soluble polymer can form ternary complexes which result in several fold increase in the water solubility of the drug. Interestingly, literature reports showed an attempt of binary complexation with derivatives of CD (*apart from SBE- β -CD*), which were independently shown to be toxic to the ocular cells thus prompting the ocular safety of SBE- β -CD.

Therefore, our strategy included the utilization of SBE- β -CD, and polyvinyl alcohol (PVA, **Fig. 1C**) to form a binary or a ternary complex of CsA, which could produce a clear solution upon solubilisation in aqueous medium. To the best of our knowledge, this is the first-of-its-kind formulation in the field of eye drops, and particularly formulating CsA aqueous formulations. In the study, the possibility of binary and ternary complexes was investigated by both *in silico* (molecular modelling, and dynamics study), and wet lab experiments. The complexes were characterized for their physicochemical properties (solubility, spectroscopy, thermal and crystallinity), morphology, *in vitro* and *ex vivo* release and permeation, biocompatibility and cytotoxicity in human ocular cells. Additionally, a detailed performance evaluation of the product was carried out using mouse models of DED, followed by slit lamp imaging, fluoresce staining, tear volume assessment, and histology. An overall workflow of the present study is presented in **Fig. 2**.

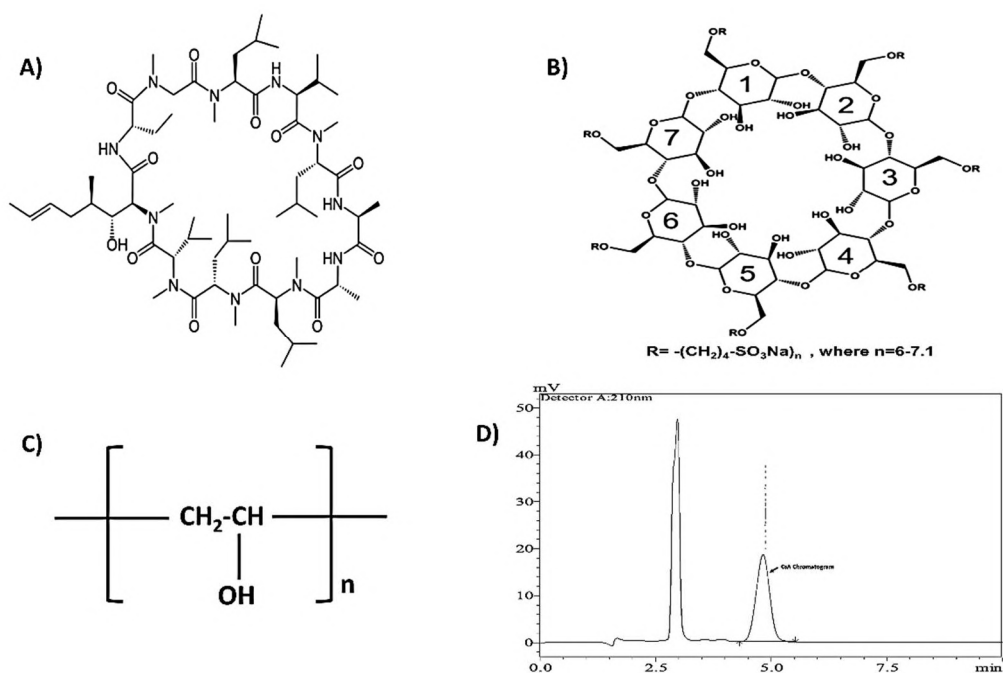


Fig. 1: Chemical structures of (A) CsA, (B) SBE-β-CD, and (C) PVA, and the representative chromatogram of CsA quantified using RP-HPLC

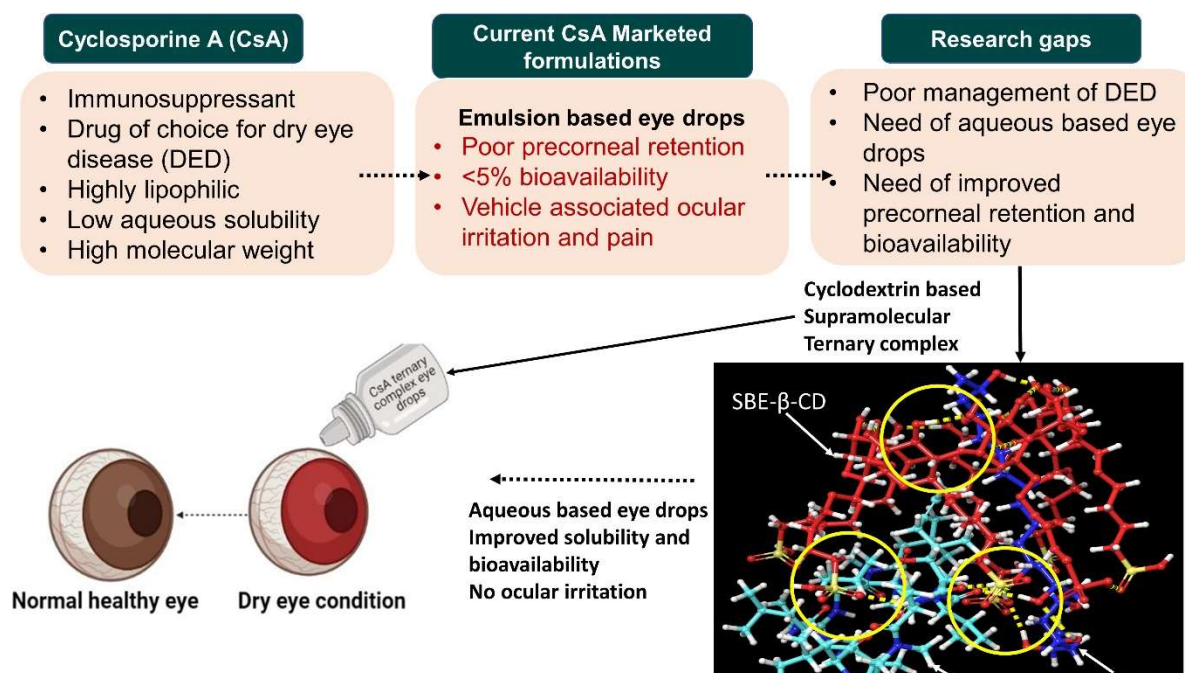


Fig. 2: Overview of the present study

2. Objectives

1. *In silico* modelling and wet-lab optimization of CsA-SBE- β -CD based binary and ternary complexes
 2. Characterization and *in vitro/ ex vivo* evaluation of the optimized complexes and formulation of eye drops
 3. *In vivo* performance evaluation of the developed CsA eye drops in scopolamine-induced mouse models of DED
-

3. Materials and methods

3.1. Materials

Cyclosporine A was received as generous gift sample from Cipla Ltd (Mumbai, India), Sulfobutylether β -CD was kindly gifted by CyDex Pharmaceuticals, Inc (USA), poly vinyl alcohol (PVA) was purchased from TCI chemicals. All other chemicals and reagents were of analytical grade and used in the study without further purification.

3.2 Animals

The study protocol was approved by the Institutional Animal Ethics Committee (IAEC), Kasturba Manipal College KMC, Manipal Academy of Higher Education (MAHE), Manipal [IEAC/KMC/17/2018]. Swiss Albino female mice weighing 30 - 40 g were procured from the Central Animal Research Facility (CARF), Manipal for the study and housed according to the institutional guidelines.

3.3. Phase solubility

Prior to the initiation of the studies, a reverse phase high performance liquid chromatography (RP-HPLC) method was developed for the quantification of CsA in both the analytical samples. The method was developed as per the reported procedures, and in our study the linearity was found to be in the CsA concentration range of 0.05 – 10 $\mu\text{g/mL}$ ($N = 3$, $R^2 > 0.993$), at 210 nm. The retention time was 4.9 min as shown in **Fig. 1D**.

To measure the increase in the solubility of CsA in CsA-SBE- β -CD complex (also referred to as **binary complex**), the phase solubility studies were carried out by Higuchi and Connors method⁷. Briefly, the procedure involved the addition of an excess amount of CsA (30 mg) to different concentrations of SBE- β -CD (0 – 40% w/v in Milli-Q water). The CsA-SBE- β -CD-PVA complex (also referred to as **ternary complex**) phase solubility was carried out similarly with keeping PVA concentration constant at 0.5%. The dispersions were sonicated at 50 ± 2 °C in a water bath sonicator for 1 h. The dispersions were allowed to cool to room temperature and to attain equilibrium. After equilibrium, samples were kept for continuous rotation (Rotospin) at 50 rpm for 72 h⁸. At the end of 72h, the samples were centrifuged (Sigma 3-30K Superspeed Refrigerated Centrifuge) at 20,000 rpm for 45 min. The supernatant was then injected into the HPLC to quantify CsA. The apparent stability constant and complexation efficiency was calculated from the phase solubility diagram using following equations.

$$K_c = \frac{Slope}{S_0} (1 - Slope) \quad \text{Eq. 1}$$

$$CE = K_c \times S_0 \quad \text{Eq. 2}$$

$$\text{Molar ratio} = \text{Drug: CD} = 1: \left(1 + \frac{1}{CE}\right) \quad \text{Eq. 3}$$

Where, K_c is the stability constant and S_0 is the solubility of CsA in the absence of SBE- β -CD.

3.4. Molecular modelling and Dynamics

In silico molecular modelling studies between CsA and SBE- β -CD was carried out using the software provided by Maestro® module (Version 11.7, Release 2018-3) available under the Schrodinger Small-Molecule Drug Discovery Suite, Schrodinger, LLC, New York. CsA structure was obtained from protein data bank (PDB ID 1IKF) which was further optimized by LigPrep and Epik module to generate energy minimized and ionization state at pH 7.4. On the other hand, SBE- β -CD was developed as per our previous reported procedures⁸. Similarly, PVA was constructed using ChemDraw Software and used in the

study. The molecular docking was carried out using the energy minimized structures of CsA, SBE- β -CD, and PVA under the Glide module after generating the grid⁹. The scoring of the generated poses was done in the extra precision mode, and the solvent-accessible area was used to calculate the change in the free energy. Further, the binding affinity was calculated using Prime MM-GBSA module, and the non-covalent forces (columbic energy, van der Waals, hydrogen bonds, and lipophilic energy) involved in complexation as per **Eq. 4**.

During the *in silico* studies, the Embrace module was used to calculate the change in free energy after complexation in two modes. In the 'energy difference mode' (Del E, **Eq. 5**), the energy calculations were performed for SBE β CD, CsA, binary and ternary complexes, including the relaxation parameters. On the other hand, the 'interaction energy mode' presented the energy resulting from the interaction of various atoms of SBE β CD and CsA and PVA as a complex, omitting their contributions.

$$\Delta G = E_{_KTZ-SBE\beta CD_M} - E_{_KTZ_M} - E_{_SBE\beta CD_M} \quad \text{Eq. 4}$$

$$Del E = E_{_KTZ-CD} - E_{_KTZ} - E_{_SBE\beta CD} \quad \text{Eq. 5}$$

The molecular dynamics (MD) were run using the Desmond module (Version 11.7, Release 2018-3). The binary and ternary complexes were immersed in simulation box individually with a 10 Å thick solvent layer following the TIP4P explicit water model and subjected to 20 ns MD simulations. The MD simulations were carried out at default settings at 300 K temperature and 1.013 bar pressure maintained using the Nose-Hoover Chain thermostat and Matryna-Tobias-Klein barostat, respectively. The MD trajectory was generated and analyzed to calculate the root mean square deviation (RMSD) plots and number of hydrogen bonds plots to study the stability of the formed complexes.

3.5. Preparation of complexes of CsA-SBE β -CD-PVA: DoE approach

In the study, the design of experiment approach (DOE) was used to optimize the formation of CsA complexes. A randomized factorial multilevel categoric design using (Design expert, Version.10.0.1.0; Stat-Ease Inc.) was optimized to evaluate the effect of different critical factors such as temperature, SBE- β -CD and PVA concentration on the aqueous solubility of CsA by selecting solubility as the response. The factors and respective levels

were selected based on the preliminary trials carried out with one factor at a time study. During preliminary trials, it was observed as reported in literature that high temperatures lead to the increase in drug solubility¹⁰. A total of 30 trials were produced by the design. Statistical analysis of variance, ANNOVA test was performed to assess the significance (p value) and impact (model F-value) of each factor selected in the design and their interactions. The optimized batch were further taken for the preparation of the binary and ternary complex by freeze drying technique.

Table 1: The various factors studies at different level to optimize the randomized factorial multilevel categoric design for the preparation of binary and ternary complexes

Factors	Number of levels	Levels						Response
Temperature (°C)	02	100			120			CsA solubility
PVA (%)	03	0		0.5	1			
SBE- β-CD (%)	05	1	2	5	7.5	10		

3.6. Preparation of Complex: Lyophilization technique

The optimized complex was prepared by lyophilization technique. Briefly, CsA and SBE- β -CD were taken in 1: 1 molar ratios. Adequate PVA was added in the solution and heated at 90 °C for 45 min. The obtained samples were kept at room temperature overnight for cooling down and to attain the equilibrium. The samples were centrifuged (3K30, Laborzentrifugen Sigma), at 15000 rpm and supernatant was collected. The collected supernatant was lyophilized to obtain the complex¹¹.

3.7. Characterization of optimized complexes

The morphology of the individual ingredients and the complexes were investigated using the FE-SEM (JEOL-JSM5800LV, Japan) while the elemental composition was measured using the Energy Dispersive X-ray Spectroscopy (EDS) in the same instrument. The surface elemental composition and their binding energies were determined using the X-ray Photoelectron Spectroscopy (XPS, Axis Ultra, Kratos Tech, UK). The thermal analysis

of the materials was carried out using Differential Scanning Calorimetry (DSC, DSC-50, Shimadzu, Japan) in the range of 25 to 300°C, and the crystallinity study was carried out using X-ray Diffraction technique (X-ray Diffractometer, Rigaku SmartLab, Tokyo) at a 2θ from 10° to 80° at a rate of 2°/ min. The functional group analysis during the formation of complexes were carried out using the Fourier Transform Infrared Spectroscopy (FTIR, FTIR-8300, Shimadzu) in the wavelength range of 4000 – 8000 cm^{-1} . The ^1H -Nuclear Magnetic Resonance (^1H -NMR) spectra was recorded on a 500 MHz Bruker Advance Neo) after dissolving the samples in D_2O : DMSO-d_6 (1:1).

3.8. Formulation of eye drops

The aqueous CsA eye drops were prepared using the PVA as vehicle. The adequate lyophilized complex was added in 3% PVA solution to prepare 0.012% and 0.04% of CsA eye drops of binary and ternary complex respectively. The samples were shaken until homogenous solution was obtained followed by heating at 60°C for 20min. Samples were cooled down at room temperature and kept overnight for equilibrium and to obtain clear solution. Vehicle control was prepared using 3% PVA and 7.5% SBE- β -CD using the same procedure.

3.9. Cytotoxicity and Biocompatibility studies

The cytotoxicity of the individual ingredients and the eye-drop formulations were evaluated by the 3-[4,5-dimethylthiazol-2-yl]-2,5-diphenyltetrazolium bromide (MTT) cleavage assay in immortalized human corneal epithelial cells (HCEC) 10.014 pRSV-T as per the standard protocols. Briefly, cells were grown to confluency and compounds were added in triplicate and incubated for 24 h. At this point, supernatants were removed, and cells were further incubated in medium containing MTT for 2 h at 37 °C. Supernatant was discarded and DMSO was added to dissolve the formazone crystals and absorbance was recorded at 570 nm. Untreated cells served as a control in the study¹².

The ocular irritation potential of the optimized binary and ternary complex was investigated in ex-vivo (in-ovo) using HET-CAM assay technique as reported earlier¹³. Freshly fertilized Fertile White Leghorn chicken eggs were procured from the local hatchery and cleaned with tap water to remove dirt. Eggs were candled to discard

defective eggs and followed by incubation for 9 days in a humidified bioincubator at 37.5°C. The eggs were rotated manually thrice a day during incubation to prevent embryo adherence to the shell membrane. On the 9th day of incubation, eggs were candled to confirm the development stage by observing the embryo and CAM blood vessels through the illuminated shell. A small window was made by removing shell and inner membrane to expose the CAM. Test sample solution (~300µL) were instilled on the exposed CAM. The reactions on CAM such as any haemorrhage, vascular lysis and coagulation was observed at different times over a 300sec (5min) after instillation of the test solution and documented. The 0.9% NaCl was used as a negative control and 1M NaOH as a positive control.

3.10. *In vitro* release profile

The in vitro dissolution pattern and release of the drug from the complex was carried out for 24 h using Franz diffusion assembly of receptor volume 5 mL. The release study was carried out using dialysis membrane (polyether sulfone, MDI Membrane Tech., India) of 0.45-µm pore size with surface area of 1.5 cm². The CsA pure drug, binary complex, and ternary complex lyophilized powder equivalent to 1mg CsA was dissolved in water and added in the donor compartment whereas receptor compartment was filled with simulated tear fluid (STF, 6.8 g sodium chloride, 2.2 g sodium bicarbonate, 0.084 g calcium chloride dehydrate, 1.4 g of potassium chloride in 1L of pure water) at 37°C and 400 rpm to mimic the ocular temperature. At predefined time intervals samples were collected and replaced with the equal volume of fresh STF media. The collected samples were centrifuged before analysing the same by developed -HPLC method for quantification of CsA.

3.11. *Ex vivo* transcorneal permeation

The *ex vivo* transcorneal permeation of CsA permeation from complexes were evaluated using freshly excised goat eyeballs procured from the local slaughterhouse as reported earlier¹⁴. Briefly, the corneal membrane was isolated carefully without any damage from the excised eyeballs of a goat and washed with normal saline. The corneal membrane was mounted on donor compartment of Franz diffusion apparatus such that the corneal epithelium faces the donor compartment whereas and receptor compartment was filled

with STF maintained at 37 °C which was continuously stirred for 24 h. The samples were added to the donor compartments after attaining equilibrium. At pre-defined time interval, 1 mL samples were collected, and equal volume of fresh media was replaced to the receptor compartment. The samples collected were centrifuged and CsA was quantified using developed RP-HPLC. The graph was plotted between cumulative drug permeated ($\mu\text{g}/\text{cm}^2$) and time and steady state flux (J_{ss}) and permeation coefficients (K_P) were calculated for each tested formulation as reported earlier¹⁵.

3.12 *In vivo* efficacy studies

3.12.1 Experimental dry eye disease mouse model

Experimental dry eye disease mouse model was developed in 5-6 weeks old female Swiss Albino mouse¹⁶. Briefly, 0.5 mg/ 0.2 ml of scopolamine hydrobromide (SABr) (TCI Chemicals) was subcutaneously injected in the alternate hindquarters four times a day to inhibit the pharmacological aqueous tear secretion for 10 days. The successful establishment of the dry eye model was evaluated by measurement of tear volume, slit lamp microscopic imaging with corneal fluorescein staining and histopathological evaluation. The cornea, extra orbital lacrimal gland (LG) and harderian gland (HG) were extracted and fixed in 10% buffered formalin for further processing. Blocking or embedding the tissue was done to transfer the tissue from the final wax bath to a mold filled with molten paraffin wax. Thin sections of tissues block of 4 microns were cut with the help of microtome. The slides were stained with H & E (Haematoxylin and Eosin) observed under the LX-500 LED trinocular Research microscope (Labomed) and images were taken with MiaCam CMOS AR 6pro microscope camera connected to image AR pro software.

3.12.2 *In vivo* efficacy studies in dry eye mouse model

After successful establishment of dry eye disease mouse model, mice were randomized into six groups with each group having six animals. The mice were treated with marketed formulation (CsA eye drops (0.05%)), binary complex eye drops (0.012%), ternary complex eye drops (0.04%) and vehicle control. Two groups were evaluated as normal control and diseased control. The treatment was given twice a day with 12 h interval for

10 days. The efficacy of the given treatment was evaluated by measuring tear volume, slit lamp microscopic imaging with corneal fluorescein staining and histopathological evaluation.

3.12.3 Tear volume measurement

The successful induction of the model and recovery was evaluated by evaluating tear volume measurement using Schirmer tear strips (Tear Touch Blu®). The tear volume production from both eyes were measured at 1min and 5min interval every day during disease induction period followed by measuring the wet strips length as reported earlier¹⁷.

3.12.4 Slit lamp microscopic imaging

Slit lamp microscopic imaging with 1% sodium fluorescein strips (Fluoro Touch®) staining with and without cobalt blue light were taken using portable slit lamp (Keeler PSL One, Malaysia) attached with image capturing device. The white light images were captured without cobalt blue light¹⁸. The corneal staining using sodium fluorescein is a potential technique to assess the corneal damage associated with the dry eye disease.

3.12.5 Histopathological analysis

The animals from each group were sacrificed at 10th day of the treatment for the histological examination. The cornea, extra orbital lacrimal gland (LG) and harderian gland (HG) were extracted and fixed in 10% buffered formalin for further processing. The samples were processed further for H&E staining as mentioned in the **Section 3.12.1**.

3.13 Statistical analysis

The results of all the experiments were represented as the mean \pm standard deviation (SD) by performing the experiments in triplicates unless otherwise mentioned. The analysis of variance (ANOVA) was carried out to compare the two groups. A p-value of < 0.05 was considered statistically significant.

4. Results and Discussion

4.1 *In silico* molecular modelling studies

The molecular docking studies generated numerous poses for the binding of CsA to SBE- β -CD forming an inclusion complex. The contribution from different forces in formation of complex is provided in the **Table 2**. However, the best-docked pose was selected based on the docking score and binding energy obtained. As seen from the **Fig. 3**, the molecule CsA was interacting with the terminal portions of the SBE- β -CD, predominantly in the regions with the presence of sulfobutylether groups. The observed interaction is evident from the bulkiness of the CsA molecule when compared to the SBE- β -CD. Several types of interactions occurred between the guest (CsA) and the host (SBE- β -CD) enabling a calculation of the binding energy and the fitness functions. The interactions arising from the positively charged amine groups of CsA and the negatively charged groups of SBE- β -CD enabled the formation of inclusion complex. There were no interactions noted for the involvement of glucopyranose unit of SBE- β -CD clearly indicating the non-penetration of the CsA into the cavity of SBE- β -CD. Instead, the bulk of CsA was found hanging at the cavity of the seven-sulfobutylether ether chains. The visualization of the docked poses depicted an interaction of the SBE- β -CD with CsA to be partially due to the hydrogen bonding and van der Waals's interactions.

Table 2: The docking energy and other energies involved in formation of binary complex and ternary complex for the best identified pose

Complex	Docking score	ΔG Bind	ΔG Bind Colomb	ΔG Bind H Bond	ΔG Bind Lipo	ΔG Bind vdW
Binary	-1.67	-42.78	-14.15	-1.97	-14.92	-26.71
Ternary	-12.285	-76.57	-31.47	-3.69	-30.18	-46.95

Binding energy for the inclusion complex was measured in terms of ΔG based. The observed docking score was -1.67 and -12.285 for binary complex and ternary complex respectively for best identified pose from several obtained complex poses indicating that out of several poses generated while docking the selected pose was more favourable to

be formed upon successful complexation. The docking results showed a major contribution of the van der Waal's interaction than the other types of interaction to form a stable inclusion complex between CsA and SBE- β -CD. Energy calculations showed improved binding energy for the ternary complex complex which is in accordance with the experimental stability constant (K_c) obtained from phase solubility studies. The improved binding energy might be attributed to the increased contribution of van der Waals and electrostatic interactions extended by PVA. The PVA stabilized the supramolecular ternary complex by formation of bridged interactions with both CsA and SBE- β -CD-PVA observed during molecular docking studies. The docking pose obtained during binding studies were in accordance with the observed FTIR and NMR characterization of the complexes.

The improved aqueous solubility and complexation efficiency during phase solubility can be corroborated with increase in hydrophilic surface area upon formation of binary complex and ternary complex (**Fig 4A**). Hydrophilic surface area was improved in both binary and ternary complex from 316.99 cÅ in case of CsA to 1069.95 cÅ and 1007.66 cÅ, respectively. The principle of the simulations was to simulate the movement of the atoms according to the Newton's law of motion until a stable conformation of the inclusion complex was obtained. To assess the stability of the obtained docking poses the simulation was run. The structure trajectory obtained for SBE- β -CD atoms and CsA during MD simulations were aligned and root mean square deviation (RMSD) was calculated for the SBE- β -CD and CsA. The observed RMSD was within 2 Å indicating the formation of a stable structure and is likely to be formed when the experiments are conducted in wet lab. Similarly, the RMSD calculations were carried out for the ternary complex also suggested formation of stable complex as observed RMSD was within 2 Å (**Fig. 4B and 4C**). The H-bonds plot taking place during the 20 ns between the individual molecules were plotted. H-bonds plot suggests the formation of higher number of hydrogen bonds in ternary complex compared to the H-bonds in binary complex (**Fig 4D and 4E**). The interaction of PVA with SBE- β -CD and CsA was observed in docking poses. PVA forms multiple bonds with the SBE- β -CD and CsA which can aid in stabilization of formed complex.

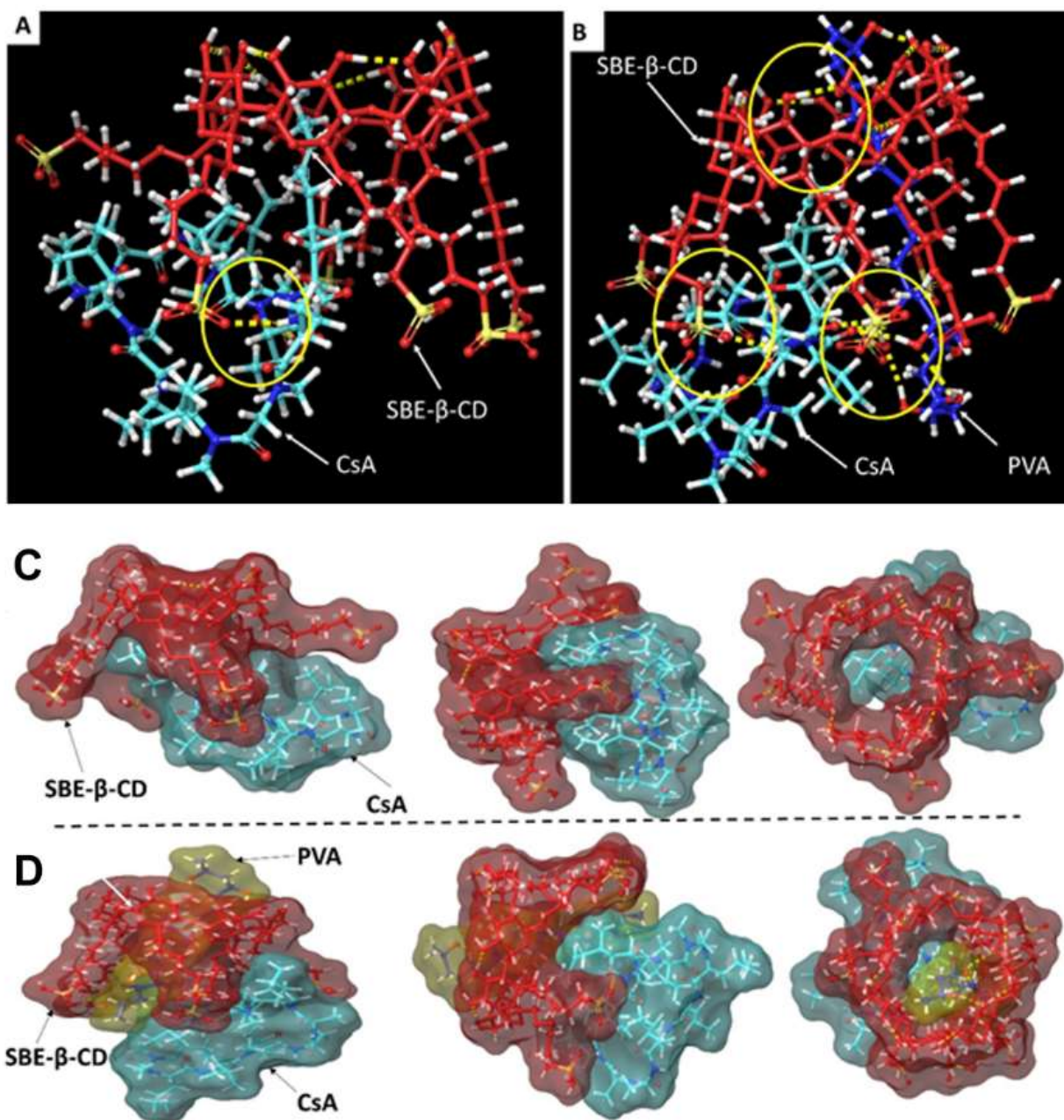


Fig. 3: Molecular modelling poses of CsA binary complex (A) and ternary complex (B) showing the interactions between CsA, SBE- β -CD and PVA; (C) and (D) showing the tight binding positions of the binary and ternary complexes (top, side and bottom view)

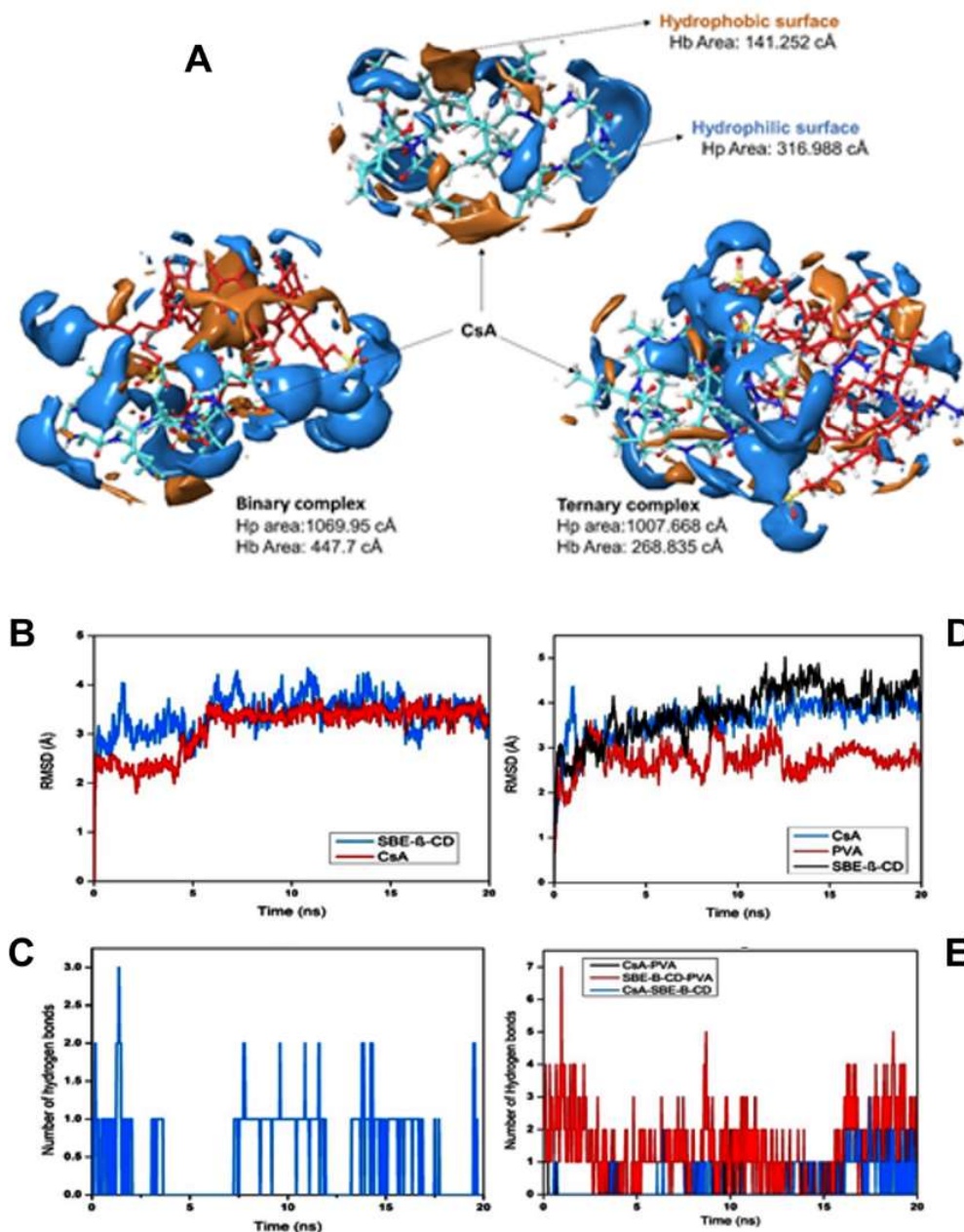


Fig 4: Hydrophilic (blue) and hydrophobic (brown) surface area (A) of CsA alone, and in binary and ternary complexes; RMSD and Hydrogen bond numbers plots generated during the molecular dynamics simulations for a duration of 20 ns. B/C and D/E represent the RMSD and hydrogen bond (H Bond) numbers values for the binary and ternary complex respectively.

4.2 Phase solubility

Stability constants (K_c) and complexation efficiency (CE) were calculated from the phase solubility studies. The phase solubility profiles of CsA with various SBE- β -CD exhibited fairly linear increase of CsA solubility as function of SBE- β -CD concentration over the varied concentration range studied up to 40 mM. However, binary complex phase solubility profile showed A_N type solubility profile suggesting SBE- β -CD is proportionally less effective at higher concentration, whereas ternary complex phase solubility profile exhibited A_L type solubility profile suggesting linear increase of drug solubility with increase in CD concentration¹⁹ (**Fig 5A**). The observed stability constant was 94.28M^{-1} and 1035.5M^{-1} for binary complex and ternary complex, respectively. The complexation efficiency (CE) for binary and ternary complex was 0.0016 and 0.0186 respectively. The stability constant ranging from 50-2000 indicates favourable interaction between drug and CDs and formation of the stable inclusion complex. The study overlaps with the previously reported literature where various parent (γ -CD) and modified CDs (RM- β -CD, HP- γ -CD and HP- α -CD) on the solubility of CsA except SBE- β -CD. The study suggested A_L type of solubility profile for all the CDs except α -CD which was in contrast to obtain A_N type of solubility in our study with SBE- β -CD²⁰. To the best of our knowledge, CsA and SBE- β -CD complex is not studied so far. However, the type of solubility profile is also dependent on the range of CDs concentration studied and hence vary in reported literature.

The molar ratio of drug and CD plays crucial role in formulating the dosage form. The solubility of CsA with and without CDs along with PVA is shown in the **Fig 5B**. The CsA is a neutral molecule whereas SBE- β -CD carries negative charge which might be affecting the inclusion complexation. In the literature, γ -CD are reported to increase the CsA aqueous solubility by formation of CD-aggregation by arranging as micelles. Also, the reports suggesting the formation of complex aggregates or micelles upon addition of ternary agents are well reported. The addition of water-soluble polymers such as PVA during preparation of drug-CDs complex has synergistic advantages such as it decreases the CDs concentration required for drug solubilisation, improves the complexation efficiency, enables controlled drug delivery and reduces toxicity²¹.

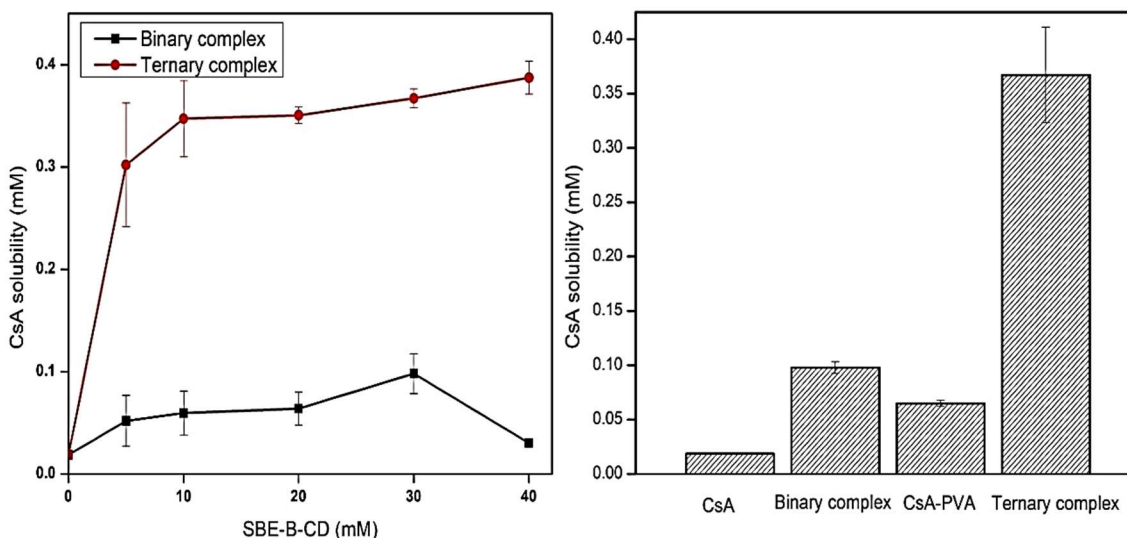


Fig 5: Binary complex and ternary complex phase solubility diagram (A) and Solubility of CsA in PVA, binary complex and ternary complex (B)

4.3. DoE approach

The implementation of design approach to systematically investigate the effect of three factors i.e., temperature, SBE-β-CD concentration and PVA concentration facilitated the identification of the potential factors on enhancing aqueous solubility of CsA. ANNOVA test results indicated that out of the three factors, SBE-β-CD concentration and PVA concentration had the significant impact on enhancement of CsA solubility and temperature and SBE-β-CD concentration together have significant impact and not individually temperature plays role. The model F-value of 14.28 implies that model is significant and there is only 0.01% chance that and F-value this large could occur due to noise. The p values which indicate the significance of model factors observed for temperature, SBE-β-CD concentration and PVA concentration was 0.7007, < 0.0001 and < 0.0001 respectively. The p values for SBE-β-CD concentration and PVA concentration observed was < 0.0500 indicates the significance of model factors whereas p values observed for temperature was > 0.1 indicates insignificant effect. It was also observed that temperature and SBE-β-CD concentration together have significant impact with p value < 0.0001. The predicted R of 0.714 and adjusted R of 0.8343 with difference less than 0.2 indicates the reasonable agreement between predicted and actual solubility data (Fig. 6A).

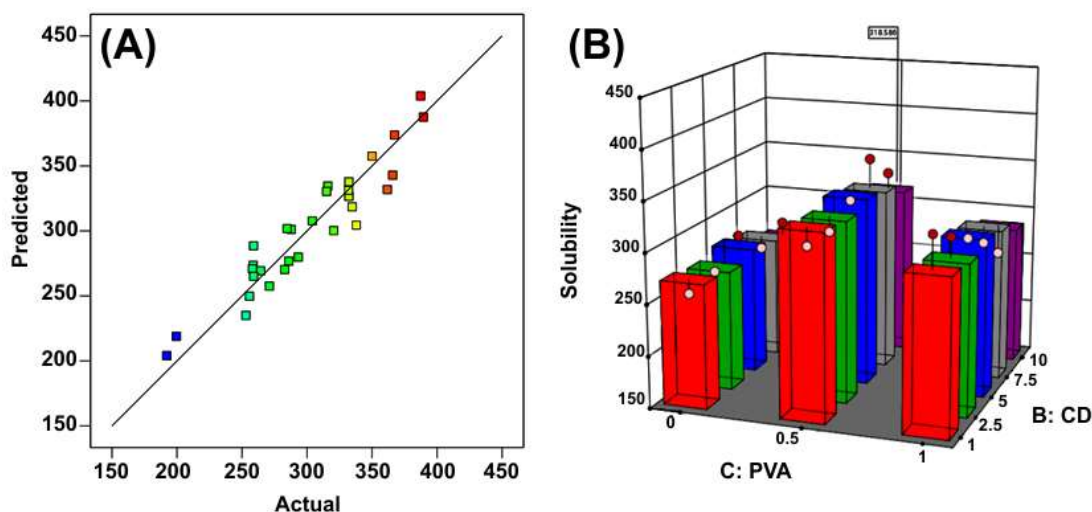


Fig. 6: Predicted v/s actual response graph (A), effect of SBE-β-CD and PVA (B)

The addition of PVA lead to the formation of ternary complexes and aggregation of which further increases the aqueous solubility of the drug. Therefore, in the complexation studies WS polymer PVA was added. It was observed that incorporation of PVA leads to significant increase in the aqueous solubility of CsA from 10-20 μ g/ mL to 350-400 μ g/mL. The optimized combinations obtained from the DoE design were compared with the actual solubility obtained and it was observed that the close agreement between the predicted and actual CsA solubility. The developed and validated DoE model can be used for predicting CsA aqueous solubility at different temperature, SBE-β-CD concentration and PVA concentration

The obtained values for the response parameters upon carrying out the preparation according to the solutions suggested were compared with the software predicted values and the relative % of error was calculated. The error for each of the responses were well below 5 % indicting a very good correlation between the predicted and the actual values. Further, the optimized batch obtained from DoE were taken to prepare CsA- SBEβCD- PVA ternary complex by freeze drying technique. It is observed that, 0.5% PVA imparts optimum increase in CsA aqueous solubility and further increase in its concentration has no significant effect. It is also observed that 0.5% PVA gives superior aqueous solubility with 7.5% SBE-β-CD compared to 10% SBE-β-CD and further increase in SBE-β-CD have no significant effect on increasing CsA aqueous solubility (**Fig. 6B**).

4.4. Characterization of Ternary complex

SEM is important tool to examine the surface morphology of resulting CDs complexes and raw materials. The SEM images of CsA appears as the rectangular crystals whereas SBE- β -CD exists as the amorphous spheres^{22,23}. In contrast, binary complex appears as the amorphous irregular particles and the original morphology of the pure CsA and SBE- β -CD disappears. The SEM of the ternary complex showed network like structure in which the binary complex is interlaced (**Fig. 7**). It is reported that polymer network increases the CDs complexation efficiency and stability of the resultant complex. The conversion of crystalline CsA to amorphous form in CDs complexes were in agreement with DSC and XRD results. The EDS characterization was carried out in conjugation with SEM for the elemental analysis. The EDS characterization revealed the elemental composition of the binary complex and ternary complex. The presence of nitrogen (N) in binary and ternary complex affirms the presence of CsA in the complex.

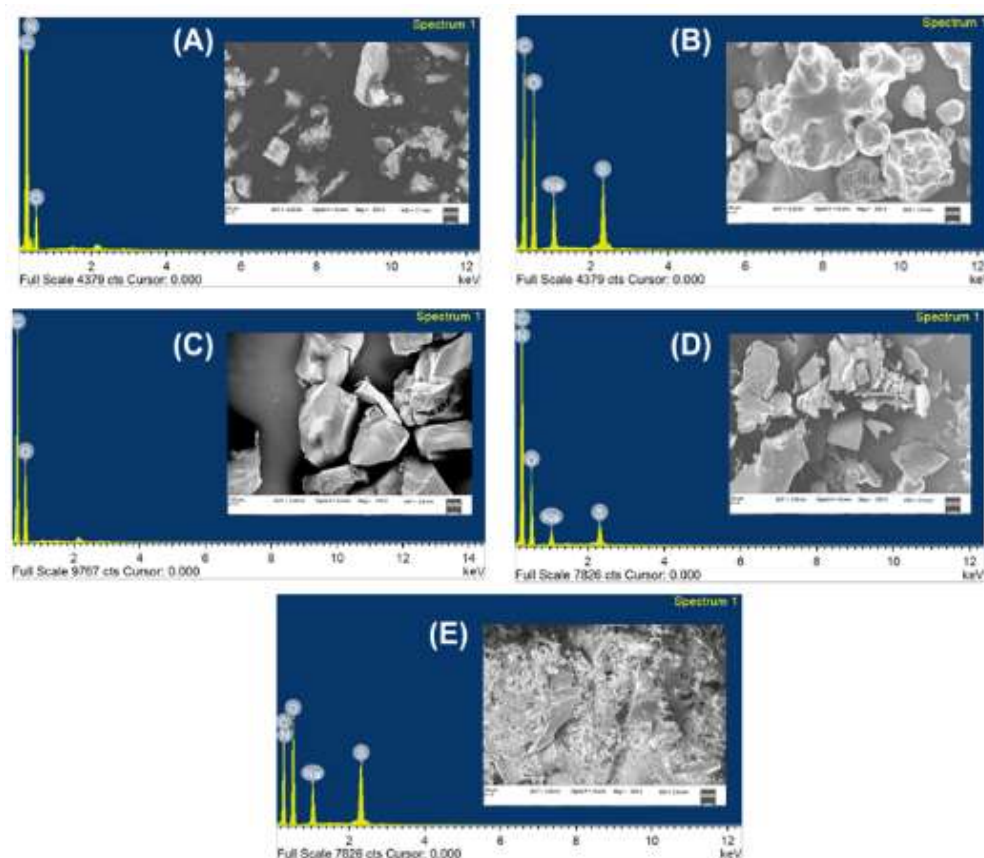


Fig. 7: FESEM images (as inserts) and EDS spectra of (A) CsA, (B) SBE- β -CD, (C) PVA, (D) binary complex and (E) ternary complex

The DSC thermogram of CsA exhibited weak melting endotherm at 127.88°C and SBE- β -CD showed broad thermal relaxation endothermic peak at 90.92°C ($\Delta H = -79.52 \text{ J/g}$) corresponding to dehydration process leading to loss of loosely bound or absorbed water molecules. The sharp endotherm at 270.51°C ($\Delta H = -45.72 \text{ J/g}$) marks the beginning of decomposition of SBE- β -CD. PVA showed sharp endotherm at 182°C confirming the crystalline nature of the PVA. In the DSC thermogram of binary inclusion complex, disappearance of the CsA typical endotherm confirms the formation of complex and conversion of crystalline CsA to amorphous form ²⁴(**Fig. 8A**). The DSC results can be corroborated by XRD results. The major peaks observed in X-ray diffractogram pattern at 9.06° disappeared in both the binary and ternary complex which affirms the CsA transition from crystalline to amorphous form (**Fig. 8B**). The formation of CDs complex with guest molecule prevents the formation of crystals and aids in transition of guest molecule from crystalline to amorphous nature.

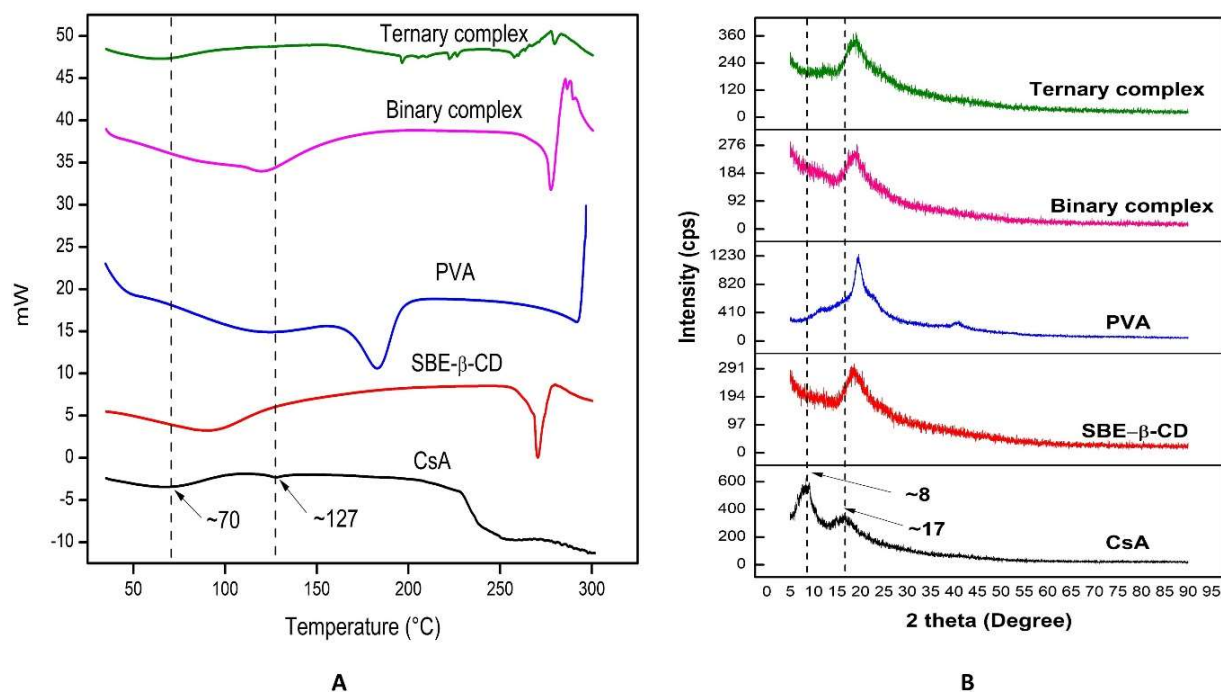


Fig. 8: DSC thermograms (A) and PXRD diffractograms (B) of pure CsA, pure SBE- β -CD, PVA, binary complex and ternary complex

XPS is the most sensitive surface characterization technique based on the basic spectroscopic principle to analyse the elemental ratio and bonding nature of the present element in the sample. The XPS spectrum provides unique peaks for each element present corresponding to specific fingerprint binding energy (eV) of the electronic configuration. The XPS plot between binding energy (eV) of the electrons on X-axis and number of electrons on Y-axis. The presence of CsA in the binary complex and ternary complex was confirmed by XPS analysis. The XPS analysis of pure was CsA carried out detecting presence of C, O and N, pure SBE- β -CD showed presence of C, O, S and Na whereas C and O in pure PVA XPS spectra (**Fig. 9**).

The host guest interactions were studied using FTIR spectra. The interactions between guest and host molecule can result in restrictions in stretching vibrations or weakening of intramolecular bonds which lead to change in shape, position, and intensity of the absorption bands. This small alteration can provide great insights into interaction between host and guest at molecular level as well as nature of the formed complex. The characteristic peaks of CsA such as intense peak at 1627.92 indicated the presence of amide stretch, secondary amine N-H stretching vibrations were confirmed by 3317, C-H stretching vibrations were observed at 2958.8 in CsA FTIR spectra^{25,26}. The prominent absorptions peaks observed in SBE- β -CD at 3365.78 indicative of presence of O-H stretch, 2935.66 represents the occurrence of alkyl stretch, 1163 stretch indicates affirms the presence of O-H group of CH₂OH, 1041 stretching vibrational peak in lower frequencies represents C-O stretch of CH₂OH. In PVA FTIR spectra, absorption bands corresponding to hydroxyl and acetate groups were observed. The prominent stretching vibrations above 3600 representing N-H vibrations, vibrations between 2840-3000 is associated with C-H stretch of alkyl group, and peaks in lower frequencies between 1730-1680 confirms the presence of C=O and C-O stretches from the acetate groups of PVA.

However, in the spectrum of binary complex and ternary complex, CsA characteristic N-H stretch of secondary amine (3317) disappeared whereas amide bending (1627.92) intensity observed was minimal, which indicates the formation of H-bonding and the interactions between SBE- β -CD and CsA in both the complexes (**Fig. 9**) The disappearance of absorption band indicates the insertion of guest molecule in host cavity of CDs. The shifting to lower frequencies of O-H stretch and C-H alkyl stretch along with

reduction in intensity in both the complexes indicates the involvement of OH group in host molecule in H-bonding. The shift in frequencies and reduction in peak intensity also indicates the breakdown of intramolecular H-bonds associated with crystalline drug observed in FTIR spectra of prepared binary and ternary complex²⁷. The FTIR interactions suggested partial inclusion of CsA in SBE- β -CD cavity and not complete inclusion as observed in molecular docking.

A stacked ¹H proton NMR spectra allowed us to compare for complex formation between SBE- β -CD and cyclosporin A (**Fig. 10**). However, a mixed solvent of D₂O: DMSO-d₆ was used to ensure improved solubility of all the components. Thus, we could clearly observe all the characteristic protons of the SBE- β -CD. CsA owing to the hydrophobic nature contributed to its limited solubility that was rather circumvented in mixed solvent system to show characteristic peak in the aliphatic domains. However, upon complexation of CsA and SBE β -CD, the characteristic CsA peaks diminished and appeared merged with the residual solvent peak that could be attributed to the aggregate formation. This is probably due to the aggregation induced signal suppression of CsA protons. The spectra for binary complex exhibited slight downfield shift for the *H*-3 and *H*-5 protons of SBE- β -CD indicating interior of CD cavity not being much affected due to complexation. However, the protons located at the exterior of the CD cavity (*H*-2 and *H*-4) and those of the sulfobutyl ether chain (*H*-4', *H*-3' and *H*-2') exhibited some downfield shift signifying involvement of charged interactions in complex formation outside the CD Cavity (**Table 3**).

Table 3: Observed chemical shift (δ in ppm) of SBE- β -CD in free state and binary complex

Protons	δ Free SBE- β -CD	δ Complex CsA- SBE- β -CD	$\Delta\delta$
H-1	4.8436	4.8520	-0.0084
H-2	3.3673	3.3846	-0.00173
H-3	3.7373	3.8114	-0.0741
H-5	3.6517	3.6632	-0.0115
H-2', 3'	1.5888	1.5942	-0.0054
H-4'	2.6438	2.6783	-0.0345

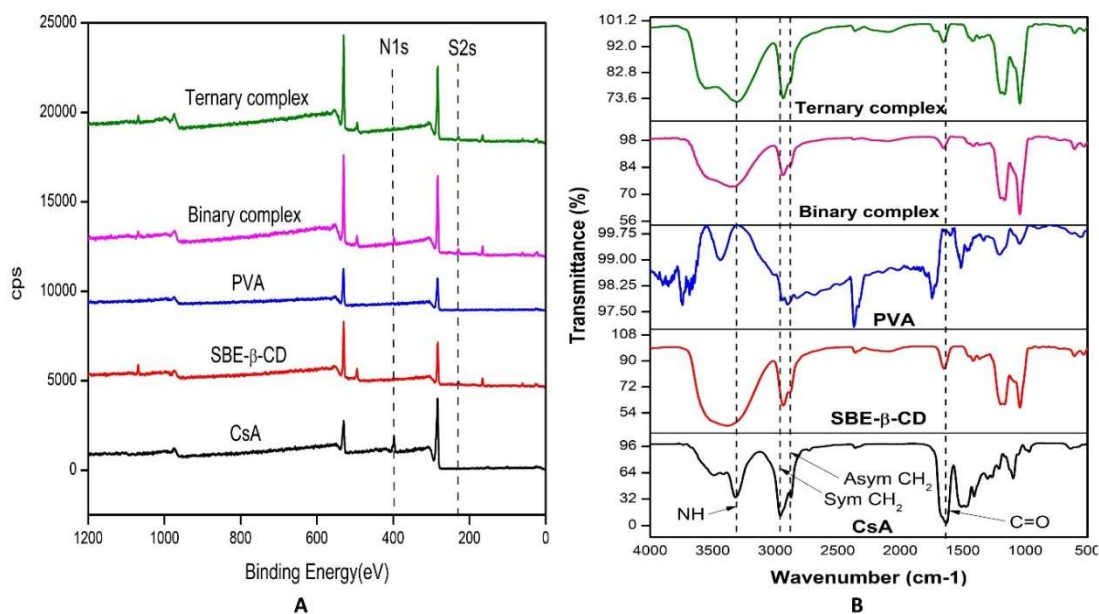


Fig 9: FTIR spectra (A) and XPS widespread energy spectra (B) for pure CsA, pure SBE-β-CD, complex CsA-CD and CsA-CD-PVA samples. The nitrogen peak is marked showing presence in pure CsA complex CsA-CD and CsA-CD-PVA samples whereas absence in the pure SBE-β-CD (Fig. 11B)

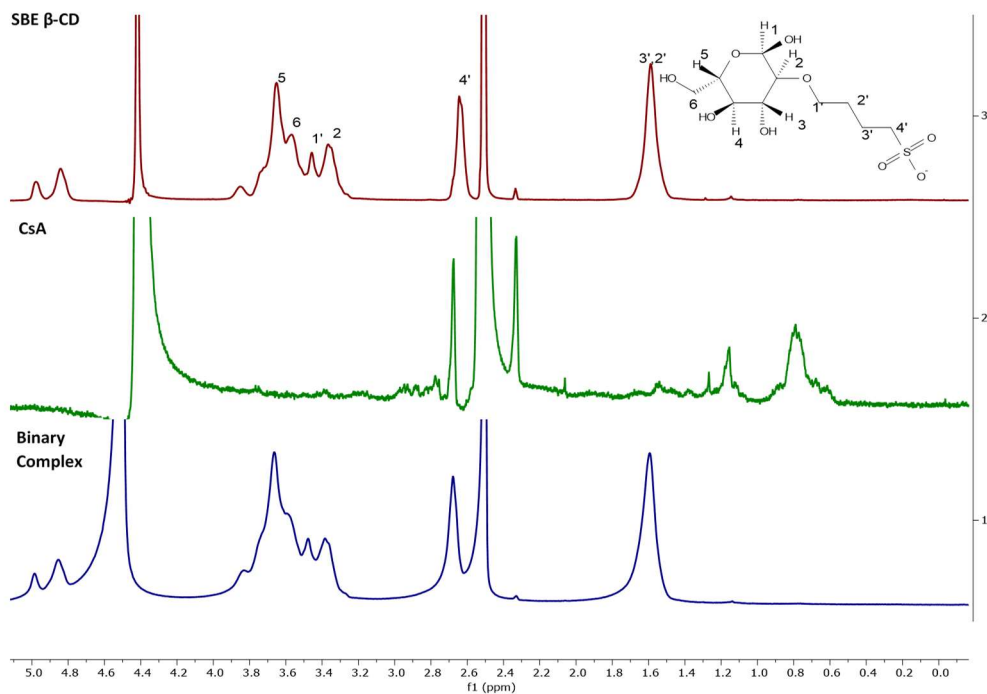


Fig. 10: Comparative ¹H NMR spectra of the SBE-β-CD, cyclosporin A and binary complex in 1:1 mixture of D₂O: DMSO-d₆. (From top to bottom) (6.5 mM)

4.5. *In vitro* release study

In vitro release studies carried out to observe the release pattern of the drug from the binary and ternary complex suggested controlled drug release from the both the complexes, in contrast to the release from the pure CsA in 24h (**Fig. 11A**). The poor drug release of the pure CsA can be attributed to the poor aqueous solubility of the drug²⁸. The formation of binary and ternary complex aided in improving the drug release compared to the pure CsA which can be attributed to the improved aqueous solubility of CsA in complex. The dilution by the aqueous media is the driving force behind the CD-drug complex dissociation. The results suggest that the CsA-CD complexation improves the dissolution behaviour of the drug compared to pure CsA. The ~3-4-fold enhancement in the dissolution profile in the binary and ternary complex can be associated with the conversion of crystalline CsA to amorphous form as suggested by the DSC and P-XRD characterization.

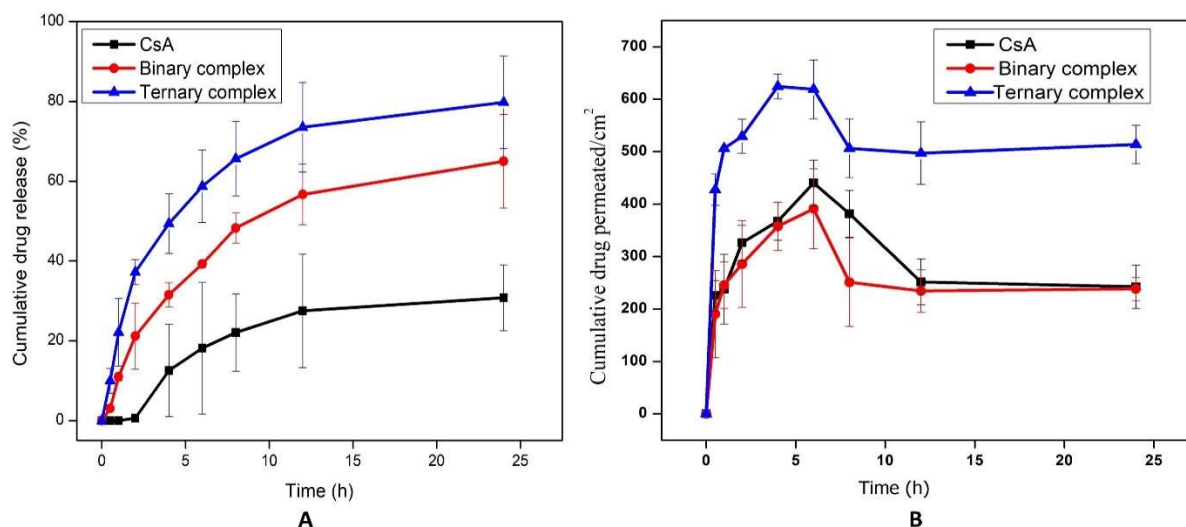


Fig. 11: *In vitro* drug release profile (A) and *ex vivo* transcorneal permeation (B) of bulk CsA, CsA- SBE- β -CD and CsA- SBE- β -CD -PVA complex

4.6. *Ex vivo* transcorneal permeation

Ex vivo transcorneal permeation suggested the significant increase in the permeation of CDs based binary complex and ternary complex composed of PVA (**Fig. 11B**). CsA- SBE- β -CD -PVA complex showed higher permeation compared to binary complex and Pure CsA, which can be attributed to the dissolved free drug available for the permeation²⁹. The *ex vivo* permeation was directly proportional to the observed solubility enhancement of the CsA in the inclusion complexes. As it was observed that ternary complex exhibited highest solubility enhancement, which suggests that the concentration of dissolved free drug available for the permeation is higher resulting in higher permeation of PVA complex followed by the binary complex and least permeation by bulk CsA. The results obtained were in accordance with the literature suggesting permeation enhancement in CDs complex based formulations³⁰. The binary complex showed improved permeation from 4h-12h compared to bulk CsA. However, permeation decreased after 12h and reached similar to bulk CsA which might be attributed to the less drug content present in the binary complex compared to CsA. The observed flux and permeation coefficient was significantly higher for the binary complex compared to the bulk CsA (Table 3).

The flux (J_{ss}) and permeability coefficient (K_p) calculated for the complexes showed similar trend with PVA complex showing highest flux. The permeability enhancement factor for binary and PVA complex was 1.63 and 1.73 respectively. Significant improvement in flux and K_p of the ternary complex was observed compared to the bulk CsA. The obtained flux, K_p and enhancement factor for both the CsA complexes are provided in the **Table 4**.

Table 4: Flux, permeability coefficient and enhancement factor of Pure CsA and CsA binary and ternary complexes

	Pure CsA	Binary complex	Ternary Complex
Flux ($\mu\text{g}/\text{h}.\text{cm}^2$)	28.5	47.65	50.71
Perm. Coefficient (cm/h)	0.019	0.031	0.033
Enhancement factor (ER)	-	1.63	1.73

4.7 Cytotoxicity and Biocompatibility studies

4.7.1 Cytotoxicity assay

The cytotoxic effect of optimized binary and ternary complex were studied on HCEC. Untreated cells were used as a normal. binary and ternary complex showed no toxicity on HCEC upon exposure for 24h. The free CsA decreased the % cell viability, however CsA in binary and ternary complex improved the % cell viability (**Fig. 12A**). The assay suggested that both complexes were practically non-irritant or nontoxic to the HCEC and can be well tolerated by ocular surface. The parent β -CD of SBE- β -CD is mild toxic to the corneal epithelium however modified SBE- β -CD is nontoxic to the corneal cells. The obtained results were in accordance with the reported literature suggesting non-toxicity of SBE- β -CD³¹.

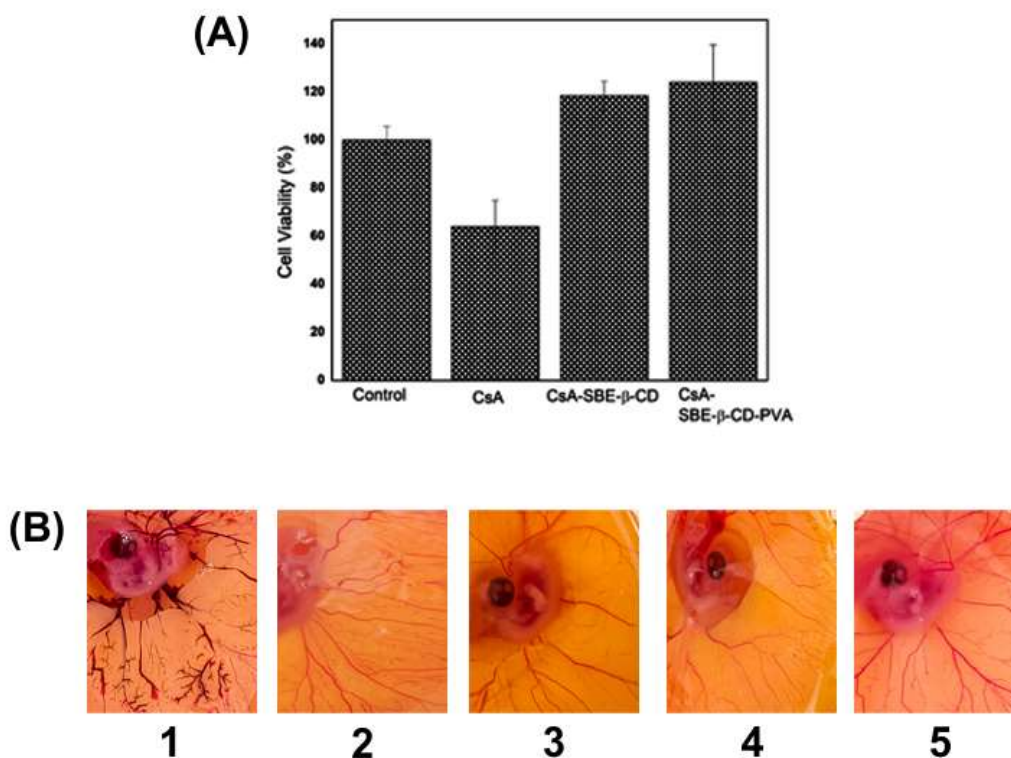


Fig. 12: % Cell viability for human corneal epithelial cells exposed to the test substances for 24h (A) and HET CAM assay (B) showing (1) positive control, (2) negative control, (3) pure SBE- β -CD, (4) binary complex and (5) ternary complex

4.7.2 HET-CAM Assay

To complement the cytotoxicity MTT assay, HET-CAM assay was carried out to assess the irritation potential of optimized binary and ternary. The potential irritant test substance can cause immediate haemorrhage, lysis, or coagulation in the blood vessels of the chorioallantoic membrane. However, both binary and ternary complex respectively showed no haemorrhage, lysis, or coagulation in the blood vessels of the chorioallantoic membrane after 5 min exposure **Fig. 12B**. The 0.1N NaOH solution employed as positive control exhibited severe haemorrhage, lysis, and coagulation of blood vessel of the chorioallantoic membrane. However, complexes were well tolerated by blood vessel of the chorioallantoic membrane suggesting the non-irritant nature of the optimized binary and ternary complex.

4.8 *In vivo* efficacy studies

4.8.1 Dry eye disease mouse model

The successful development of the dry eye disease in the mouse model was established by significant reduction in tear volume, corneal and conjunctival epithelium damage using corneal fluorescein staining and imaging as well as histopathology of cornea, lacrimal gland and harderian gland.

Sudden drop of tear volume was observed upon treatment of scopolamine when compared to the healthy control group. The observed difference between healthy control and SABr group was statistically significant and suggested an induction of dry eye disease. Corneal fluorescein imaging is potential technique to diagnose the DED which suggested the corneal and conjunctival epithelium damage. The observed corneal damage and increase in fluorescein corneal uptake attributed to the SABr mediated inhibition of tear secretion is well reported in literature^{32,33}

Histological analysis showed increase in the epithelium thickness and stromal thickness of the scopolamine treated mice compared to control group. The increase in corneal epithelium and stromal thickness observed were in accordance with that reported in literature. The increase in corneal epithelium thickness is reported in several studies associated with the abnormal proliferation and differentiation due to corneal dryness³⁴.

The LG histology in scopolamine induced group showed abundance of acute inflammatory cells such as neutrophils seen in the acini and in the connective tissue surrounding the acini. Similarly, degeneration or destruction of acinar cells were observed in the histology of both scopolamine induced and BAC induced group. The ELG histology also revealed the presence of congested blood vessels in scopolamine induced group. However, control group showed no inflammatory cells or degeneration or destruction of acinar cells in both LG and HG histology. The histology suggests that dry eye disease affects both LG and HG upon progression of the disease.

4.9. *In vivo* efficacy studies in dry eye mouse model

4.9.1 Tear volume assessment

Tear volume assessment was done during the 10 days treatment with Vehicle control, marketed formulation, binary complex eye drops and ternary complex eye drops. (**Fig. 13**). The tear production was improved in all group however significant improvement in tear volume production was observed for binary complex eye drops and ternary complex eye drops compared to untreated disease control group after 10 days of treatment. Vehicle control and marketed formulation resulted in insignificant improvement in tear volume after 10 days treatment. The improved tear volume in binary and ternary complex-based eye drops might be attributed to the prolong retention of the CsA at the ocular surface attributed to the PVA. SBE- β -CD is well reported as a drug carrier which improves the drug concentration at the ocular surface and aids in improved permeation and bioavailability of the drug³⁵. Ocular eye drops available in market suffers from poor bioavailability (<5%) attributed to the poor retention and permeation at the ocular surface.

4.9.2 Corneal fluorescein microscopic imaging

The white light and corneal sodium fluorescein-staining imaging suggested improved cornea staining when compared to the disease model. The corneal epithelium staining was not observed for marketed formulation, binary complex and ternary complex after 10 days of treatment twice a day. The absence of corneal staining and corneal damage might be attributed to the therapeutic efficacy of the marketed formulation and CsA-SBE- β -CD based optimized eye drops. The obtained results can be corroborated with the improved

tear volume. The tear volume in binary complex and ternary complex eye drops as well as CsA marketed formulation groups were very close to the healthy control group suggesting improved ocular surface condition in the dry eye mouse model. However, untreated group and vehicle control group showed presence of mild corneal staining as well corneal surface irregularities, which might be attributed to the absence of the CsA (**Fig. 14**). The observations suggested the significant role of the CsA in treatment of dry eye disease.

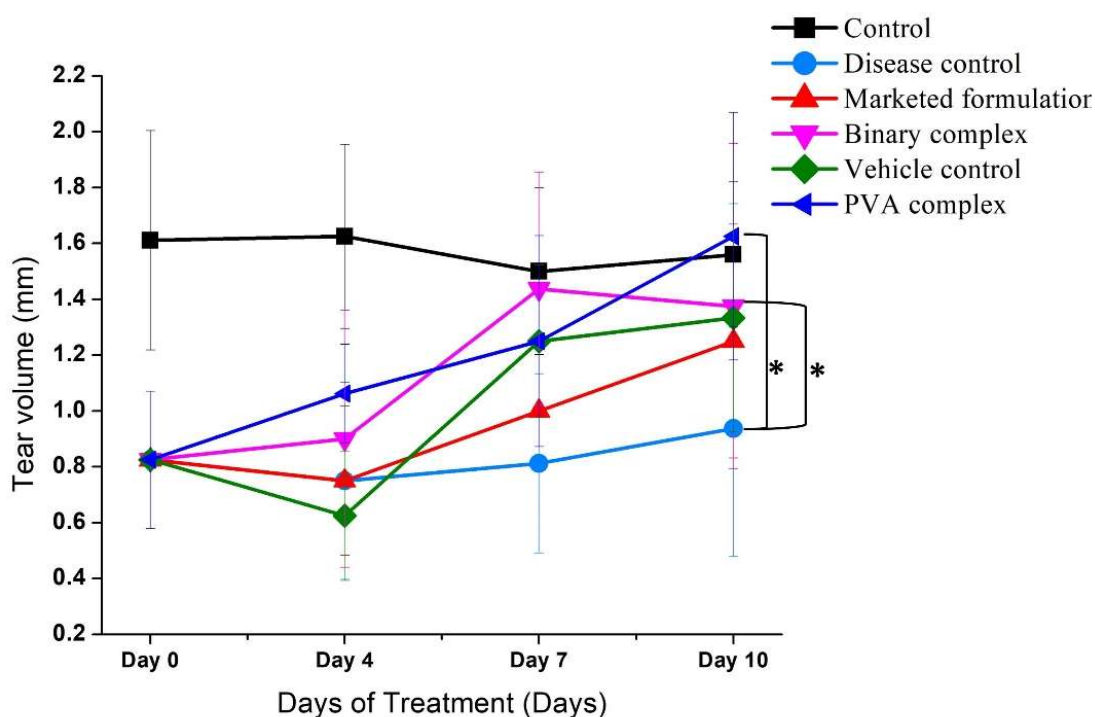


Fig. 13: Change in the tear volume in the dry eye mouse model after different treatment against the normal control and diseased control (Untreated). Binary complex and ternary complex eye drops showed significant difference against untreated diseased control whereas in marketed formulation and vehicle control group difference was insignificant however improved tear volume was observed compared to untreated after 10days treatment. showed (Each data points represents mean \pm SD, * indicates statistical significance ($p < 0.05$) between disease control (Untreated) and binary complex and PVA complex eye drops by unpaired Student t-test.)

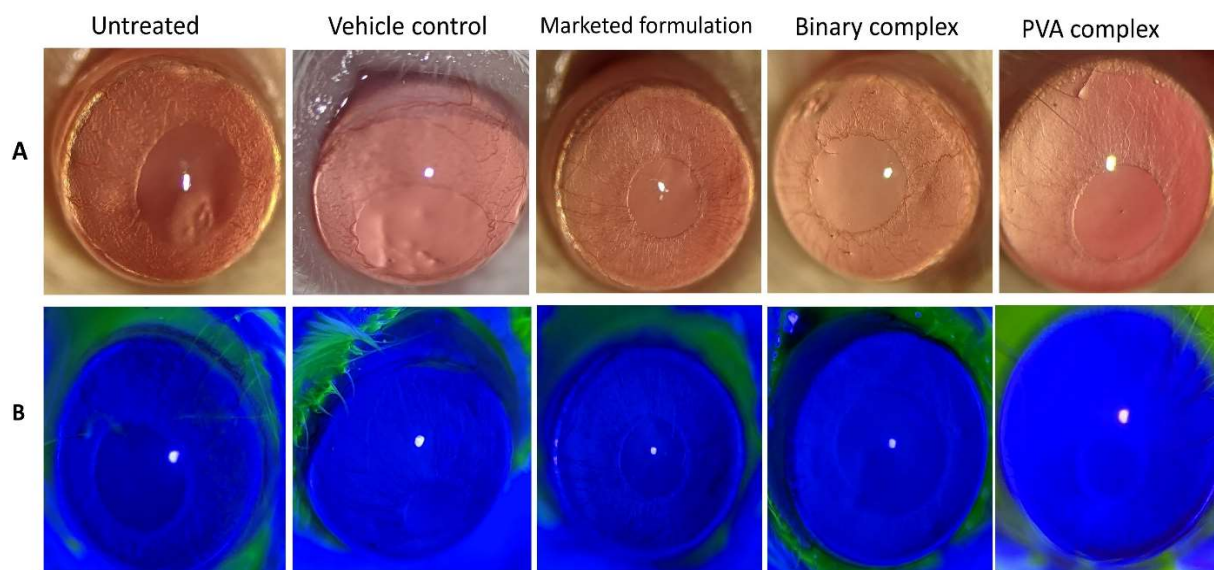


Fig. 14: Slit lamp white light (A) and corneal sodium fluorescein-stained (B) images for the untreated group, Vehicle control, marketed formulation, binary complex and PVA complex after 10 days of treatment twice a day. Untreated disease control group showed mild corneal epithelium staining and corneal surface irregularities was observed in white light imaging. Similar observations were made for the vehicle control with irregular corneal smoothness. The marketed formulation, Binary complex and PVA complex group showed corneal smoothness and no corneal staining after 10 days of treatment.

4.9.3 Histopathological analysis

The histological analysis suggested that the ternary complex eye drops successfully reduced the corneal and lacrimal gland inflammation (**Fig. 15**). The marketed formulation also showed similar effect as ternary complex in reducing the corneal inflammation however, the LG histology showed presence of both acute and chronic inflammation. The LG gland histology of untreated, marketed formulation, binary complex eye drops, and vehicle control treated group showed serous glands with many acute inflammatory cells like neutrophils around the gland. The Chronic inflammatory infiltrates and congested blood vessels were seen between the acini and few slightly dilated ducts. The vehicle control group and binary complex eye drops also showed corneal epithelial hyperplasia whereas no epithelial hyperplasia was observed in ternary eye drops group and marketed formulation group. The ternary eye drops treated group showed few acute inflammatory

cells seen surrounding the acini and no dilated glands. The corneal histology of untreated group showed edematous areas with desquamation of epithelium seen and slightly reduced epithelial thickness in some areas along with presence of inflammatory cells. In the HG histology, untreated, marketed formulation and binary eye drops group showed slightly dilated lumen and few congested blood vessels with no inflammatory cells. However, ternary complex eye drops showed congested blood vessels but did not show dilated lumen. The presence of neovascularization was observed in all groups after 10 days treatment.

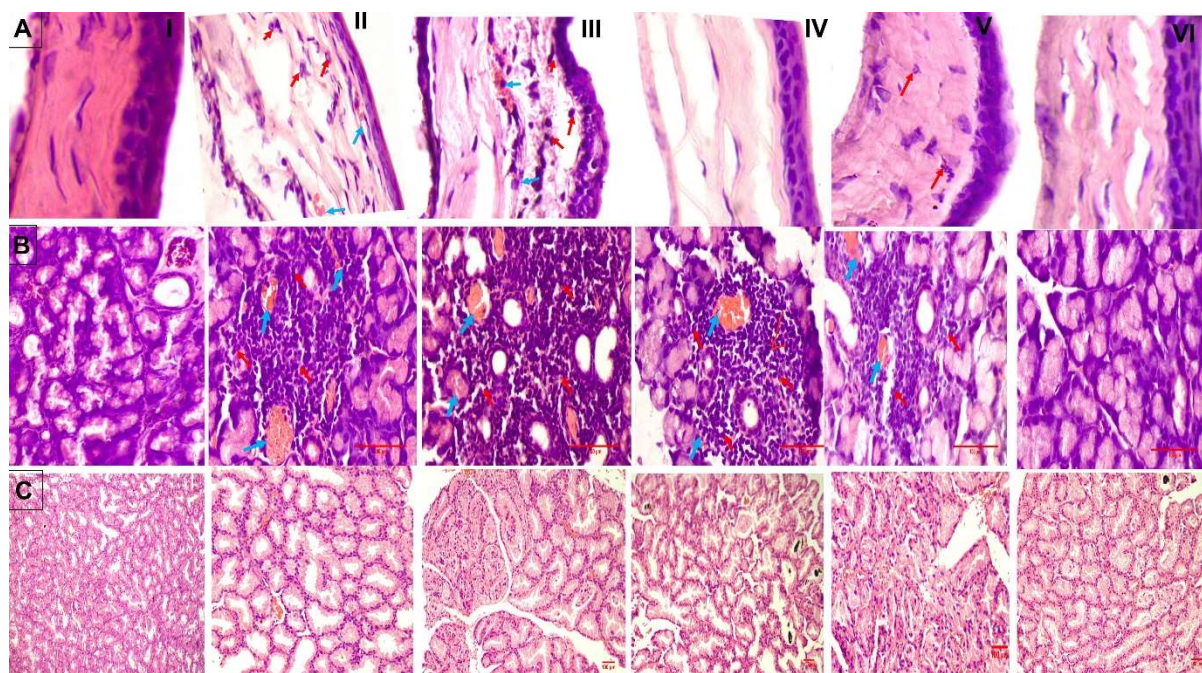


Fig. 15: H& E staining of Cornea (A), Lacrimal gland (b) and Harderian gland (C) of the Normal control (I), Untreated or diseased control (II), Vehicle control (III), marketed formulation (IV), binary complex eye drops (V) and ternary complex eye drops (VI) groups after 10 days twice a day treatment after development of dry eye disease in mouse model. Red arrow indicates presence of inflammatory cells whereas blue arrow indicated presence of neovascularization in cornea and lacrimal gland.

Overall, the presence of inflammation in cornea and LG were reduced with the treatment with optimized binary and ternary complex similar to marketed formulation. The topical treatment was started at 11th day after starting induction of dry eye model which appears to be practical as treatment is given generally after the onset of disease in clinical settings.

The histology study suggested that the Ternary complex eye drops treated group was more effective in reducing the inflammation in both the cornea as well as lacrimal gland compared to the marketed formulation and binary complex eye drops. The study suggested the superiority of the ternary complex in the treatment of the dry eye disease.

The poor recovery of binary complex (0.012%) eye drops treated group might be attributed to the lesser drug concentration compared to marketed formulation (0.05%) and ternary complex (0.04%). However, it is important to note that the ternary complex with 0.04% CsA showed superior anti-inflammatory activity and improved tear production compared to the marketed 0.05% CsA eye drops. The marketed formulation of CsA for the treatment of DED are available in concentration range of 0.05 – 1% emulsion-based eye drops.

Several studies exploring CDs to improve CsA solubility are reported to treat different ocular inflammatory conditions so far. Sasamoto *et al* studied the effectiveness of CsA- α -CD complex solution on experimental uveitis. The study suggested that topical CsA- α -CD application is effective in treating anterior uveitis but not posterior uveitis³⁶. However, the % α -CD used to solubilize CsA was not disclosed in the study. In similar study, Takano *et al*, suggested that the 0.025% CsA suppressed corneal allograft's immune reaction when administered as CsA- α -CD complex. Also, study showed 5-10 times higher corneal permeation compared to CsA eye drops in lipophilic vehicles³⁷. In another study, efforts were made to solubilize CsA with parent CDs²⁰. Study showed that α -CD improved the CsA solubility to 0.76 mg/mL at 5% and 4.22 mg/mL at 15%. Similarly, γ -CD ~0.06 mg/mL and 0.11 mg/mL at 5% and 15%, respectively. However, parent CDs (α -CD, β -CD and γ -CD) has limited water solubility and exhibits lipophilic nature which is associated with the ocular irritation due to extraction of lipids from biological membranes. Parent CDs are not approved for the ocular use and imparts ocular toxicity at lower concentrations³⁸. The α -CD imparts ocular irritation at >4%. Further, the reported studies have not explored the *in vivo* efficacy on experimental dry eye model. The modified CDs are safer and can be used at higher concentration (~10%) without causing any ocular irritation or toxicity. Our study can be a potential pavement towards development of CDs based aqueous eye drops for the topical delivery of CsA with the use of modified CDs, which are not explored so far.

Several nanocarriers based CsA ocular drug delivery has been explored so far and evaluated in different experimental dry eye model. Liu *et al* developed poly (D, L-lactide)-b-dextran loaded CsA mucoadhesive nanoparticle and evaluated in scopolamine induced experimental murine dry eye mouse model. CsA nanoparticles improved the precorneal retention time and increased the tear volume. The CsA nanoparticles further aided in elimination of inflammatory infiltrates and recovery of ocular surface³⁹. In another study CsA micellar solution was developed and evaluated in atropine sulphate induced dry eye rabbit model. The study observed improved goblet cell density and tear production upon in CsA micellar solution treated group. Yavuz *et al.* explored PLGA loaded CsA nanoparticle loaded nano decorated subconjunctival PCL implants and evaluated the *in vivo* efficacy in benzalkonium induced dry eye mouse model by surgical implantation⁴⁰. Implant showed drug release up to 90 days however, surgical implantation might not be patient friendly choice. The potential area of research for CsA delivery has been oil and surfactant-based delivery due to poor solubility and high lipophilic nature of CsA. However, those are associated with the low bioavailability and can lead to blurry vision, burning sensation, itching and ocular surface irritation. An aqueous based approach can be a potential alternative towards safer drug delivery.

The enhanced activity of ternary complex might be attributed to the improved precorneal retention and permeation offered by CDs and PVA. CDs increases the availability of the drug at the ocular surface and aids in improving the drug permeability and bioavailability.

5. Conclusion

The study explored the role of CDs and PVA in improving CsA aqueous solubility. The ternary complex improved the aqueous solubility of CsA significantly compared to the binary complex. The molecular modelling studies provided great insights in the complex formation and were in accordance with the experimental phase solubility studies and FTIR and NMR characterization results. The docking poses obtained were in close agreement with the NMR characterization and FTIR data. The DoE approach identified the critical parameters in formation of the complex which can be used to obtain the desired aqueous solubility of the drug. The ex vivo permeation study showed improved CsA transcorneal

permeation attributed to the improved drug solubility, increasing the availability of the drug at the permeation site. The cytotoxicity and biocompatibility studies suggested the optimized complexes were well tolerated and are safe for ocular use. The *in vivo* efficacy study suggested significant improvement in dry eye condition after 10 days treatment with ternary complex eye drops when compared to the marketed formulation and binary complex eye drops. The ternary complex improved overall inflammation in both cornea and LG compared to the marketed formulation and binary complex. The CDs based ternary supramolecular complex can be a safer and potential technique for improving the aqueous solubility of poorly water-soluble drugs, prolong retention at the ocular surface and improved therapeutic efficacy.

6. Impact of the Research in the Advancement of Knowledge

Ocular surface disorders, particularly dry eye disease (DED) is continuing to affect a large population worldwide, and is a growing concern among children, and young adults. Not only is the lifestyle taking a toll on the ocular health of the individual, but also the increased screen-time (for educational, scientific, and recreational purposes). Though there are numerous therapeutic modalities available in the market, a large emphasis is placed on the cyclosporine A (CsA) eye drops. As the clinical cases of DED is on the rise, an equal rise is also seen in the research directed towards a safe and effective topical ocular product. In the purview, the present study is highly relevant in terms of producing a completely aqueous and (nano)particle-free formulation, that can not only aid in the effective treatment but also be industry-friendly.

Several ocular formulations contain an oil-based system making them inherent with side-effects, reducing their clinical utility. The success of the binary and ternary complex-based eye drops is a boon for CsA and similar other molecules that are challenging to incorporate into an aqueous system. Furthermore, the use of the largely accepted cyclodextrin (SBE- β -CD) and polyvinyl alcohol (PVA) makes the formulation biocompatible, and biodegradable in nature. The result of the study also demonstrates the possibility of ternary complexes (using water soluble polymers) to form better ocular formulations, opening up avenues for the exploitation of other naturally occurring and/ or synthetic polymers for topical ocular delivery.

7. References

1. Lemp, M. A. *et al.* The Definition and Classification of Dry Eye Disease: Report of the Definition and Classification Subcommittee of the International Dry Eye Workshop (2007). *Ocul. Surf.* **5**, 75–92 (2007).
2. Stapleton, F. *et al.* TFOS DEWS II Epidemiology Report. *Ocular Surface* vol. 15 334–365 (2017).
3. Lollett, I. V. & Galor, A. Dry eye syndrome: Developments and lifitegrast in perspective. *Clin. Ophthalmol.* **12**, 125–139 (2018).
4. Utine, C. A., Stern, M. & Akpek, E. K. Clinical review: Topical ophthalmic use of cyclosporin A. *Ocul. Immunol. Inflamm.* **18**, 352–361 (2010).
5. Lallemand, F. *et al.* Cyclosporine A delivery to the eye: A comprehensive review of academic and industrial efforts. *European Journal of Pharmaceutics and Biopharmaceutics* vol. 117 14–28 (2017).
6. Siefert, B. & Keipert, S. Influence of alpha-cyclodextrin and hydroxyalkylated β -cyclodextrin derivatives on the in vitro corneal uptake and permeation of aqueous pilocarpine-HCl solutions. *J. Pharm. Sci.* **86**, 716–720 (1997).
7. Higuchi, T., Connors, K. . Phase solubility techniques. *Adv. Anal. Chem. Instrum* **4**, 117–212 (1965).
8. Shah, A. A. *et al.* Cyclodextrin based bone regenerative inclusion complex for resveratrol in postmenopausal osteoporosis. *Eur. J. Pharm. Biopharm.* **167**, 127–139 (2021).
9. M, P. & R, H. Multicomponent cyclodextrin system for improvement of solubility and dissolution rate of poorly water soluble drug. *Asian J. Pharm. Sci.* **14**, 104–115 (2019).
10. Loftsson, T. & Friirisdóttir, H. The effect of water-soluble polymers on the aqueous solubility and complexing abilities of β -cyclodextrin. *Int. J. Pharm.* **163**, 115–121 (1998).
11. Wang, Z., Deng, Y., Sun, S. & Zhang, X. Preparation of hydrophobic drugs


- cyclodextrin complex by lyophilization monophasic solution. *Drug Dev. Ind. Pharm.* **32**, 73–83 (2006).
12. Roy, S., Bonfield, T. & Tartakoff, A. M. Non-Apoptotic Toxicity of *Pseudomonas aeruginosa* toward Murine Cells. *PLoS One* **8**, e54245 (2013).
 13. McKenzie, B., Kay, G., Matthews, K. H., Knott, R. M. & Cairns, D. The hen's egg chorioallantoic membrane (HET-CAM) test to predict the ophthalmic irritation potential of a cysteamine-containing gel: Quantification using Photoshop® and ImageJ. *Int. J. Pharm.* **490**, 1–8 (2015).
 14. Mudgil, M. & Pawar, P. K. Preparation and In Vitro/Ex Vivo Evaluation of Moxifloxacin-Loaded PLGA Nanosuspensions for Ophthalmic Application. *Sci. Pharm.* **81**, 591 (2013).
 15. Zhang, F. *et al.* Ultra-small nanocomplexes based on polyvinylpyrrolidone K-17PF: A potential nanoplatform for the ocular delivery of kaempferol. *Eur. J. Pharm. Sci.* **147**, 105289 (2020).
 16. Coursey, T. G. *et al.* Dexamethasone nanowafer as an effective therapy for dry eye disease. *J. Control. Release* **213**, 168–174 (2015).
 17. Fujihara, T., Murakami, T., Nagano, T., Nakamura, M. & Nakata, K. INS365 suppresses loss of corneal epithelial integrity by secretion of mucin-like glycoprotein in a rabbit short-term dry eye model. *J. Ocul. Pharmacol. Ther.* **18**, 363–370 (2002).
 18. Wang, G. *et al.* The role of autophagy in the pathogenesis of exposure keratitis. *J. Cell. Mol. Med.* **23**, 4217–4228 (2019).
 19. Sá Couto, A., Salústio, P. & Cabral-Marques, H. Cyclodextrins. in *Polysaccharides: Bioactivity and Biotechnology* 247–288 (Springer International Publishing, 2015). doi:10.1007/978-3-319-16298-0_22.
 20. Jóhannsdóttir, S., Jansook, P., Stefánsson, E. & Loftsson, T. Development of a cyclodextrin-based aqueous cyclosporin A eye drop formulations. *Int. J. Pharm.* **493**, 86–95 (2015).

21. Liu, N., Higashi, K., Ueda, K. & Moribe, K. Effect of guest drug character encapsulated in the cavity and intermolecular spaces of γ -cyclodextrins on the dissolution property of ternary γ -cyclodextrin complex. *Int. J. Pharm.* **531**, 543–549 (2017).
22. Molpeceres, J., Aberturas, M. R. & Guzman, M. Biodegradable nanoparticles as a delivery system for cyclosporine: Preparation and characterization. *J. Microencapsul.* **17**, 599–614 (2000).
23. Kulkarni, A. D. & Belgamwar, V. S. Inclusion complex of chrysin with sulfobutyl ether- β -cyclodextrin (Captisol®): Preparation, characterization, molecular modelling and in vitro anticancer activity. *J. Mol. Struct.* **1128**, 563–571 (2017).
24. Lahiani-Skiba, M. *et al.* Enhanced dissolution and oral bioavailability of cyclosporine a: Microspheres based on $\alpha\beta$ -cyclodextrins polymers. *Pharmaceutics* **10**, (2018).
25. Al-Saedi, Z. H. F., Alzhrani, R. M. & Boddu, S. H. S. Formulation and in Vitro Evaluation of Cyclosporine-A Inserts Prepared Using Hydroxypropyl Methylcellulose for Treating Dry Eye Disease. *J. Ocul. Pharmacol. Ther.* **32**, 451–462 (2016).
26. Stevenson, C. L., Tan, M. M. & Lechuga-Ballesteros, D. Secondary structure of cyclosporine in a spray-dried liquid crystal by FTIR. *J. Pharm. Sci.* **92**, 1832–1843 (2003).
27. Adeoye, O. *et al.* Cyclodextrin solubilization and complexation of antiretroviral drug lopinavir: In silico prediction; Effects of derivatization, molar ratio and preparation method. *Carbohydr. Polym.* **227**, 115287 (2020).
28. Lallemand, F., Felt-Baeyens, O., Besseghir, K., Behar-Cohen, F. & Gurny, R. Cyclosporine A delivery to the eye: A pharmaceutical challenge. *Eur. J. Pharm. Biopharm.* **56**, 307–318 (2003).
29. Polat, H. K. *et al.* Development of besifloxacin HCl loaded nanofibrous ocular inserts for the treatment of bacterial keratitis: In vitro, ex vivo and in vivo evaluation. *Int. J. Pharm.* **585**, (2020).

30. Jansook, P., Praphanwittaya, P., Sripetch, S. & Loftsson, T. Solubilization and in vitro permeation of dovitinib/cyclodextrin complexes and their aggregates. *J. Incl. Phenom. Macrocycl. Chem.* **97**, 195–203 (2020).
31. Das, O., Ghate, V. M. & Lewis, S. A. Utility of sulfobutyl ether β -Cyclodextrin inclusion complexes in drug delivery: A review. *Indian Journal of Pharmaceutical Sciences* vol. 81 589–600 (2019).
32. Dilek Dursun, Min Wang, Dagoberto Monroy, De-Quan Li, Balakrishna L Lokeshwar, Michael E Stern, Stephen C PflugfelderDilek Dursun 1, Min Wang, Dagoberto Monroy, De-Quan Li, Balakrishna L Lokeshwar, Michael E Stern, S. C. P. A mouse model of keratoconjunctivitis sicca. *Invest Ophthalmol Vis Sci* **43**, 632–638 (2002).
33. Lee, H., Kim, C. E., Ahn, B. N. & Yang, J. Anti-inflammatory effect of hydroxyproline-GQDGLAGPK in desiccation stress-induced experimental dry eye mouse. *Sci. Rep.* **7**, 1–12 (2017).
34. Devasari, N. *et al.* Inclusion complex of erlotinib with sulfobutyl ether- β -cyclodextrin: Preparation, characterization, in silico, in vitro and in vivo evaluation. *Carbohydr. Polym.* **134**, 547–556 (2015).
35. Morrison, P. W. J., Connon, C. J. & Khutoryanskiy, V. V. Cyclodextrin-Mediated Enhancement of Riboflavin Solubility and Corneal Permeability. *Mol. Pharm.* **10**, 756–762 (2013).
36. Sasamoto, Y., Hirose, S., Ohno, S., Onoé, K. & Matsuda, H. Topical Application of Ciclosporin Ophthalmic Solution Containing Alpha-Cyclodextrin in Experimental Uveitis. *Ophthalmologica* **203**, 118–125 (1991).
37. T Takano, C Kobayashi, R M Alba, A. K. The immunosuppressive effects of 0.025% cyclosporin eye drops in alpha cyclodextrin on rabbit corneal allografts. *Nihon. Ganka Gakkai Zasshi* **96**, 834–40 (1992).
38. Chaudhari, P., Ghate, V. M. & Lewis, S. A. Supramolecular cyclodextrin complex: Diversity, safety, and applications in ocular therapeutics. *Exp. Eye Res.* **189**, 107829 (2019).

39. Liu, S. *et al.* Cyclosporine A loaded mucoadhesive nanoparticle eye drop formulation enhances treatment of experimental dry eye in mice using a weekly dosing regimen. doi:10.1021/acs.molpharmaceut.6b00445.
40. B, Y. *et al.* In vivo tissue distribution and efficacy studies for cyclosporin A loaded nano-decorated subconjunctival implants. *Drug Deliv.* **23**, 3279–3284 (2016).

Nominee : Pinal chaudhari


26/10/21